

© 2020. K.A. Farhan, M.A. Shallal.

This is an open-access article distributed under the terms of the Creative Commons Attribution-NonCommercial-NoDerivatives License (CC BY-NC-ND 4.0, <https://creativecommons.org/licenses/by-nc-nd/4.0/>), which permits use, distribution, and reproduction in any medium, provided that the Article is properly cited, the use is non-commercial, and no modifications or adaptations are made.



EXPERIMENTAL BEHAVIOUR OF CONCRETE-FILLED STEEL TUBE COMPOSITE BEAMS

KHAWLA A. FARHAN¹, MUHANED A. SHALLAL²

The main objective of this study is to highlight the performance of beams composed of lightweight concrete-filled steel tubes (square and circle sections) composite with reinforced concrete deck slab. A total of nine composite beams were tested included two circular and seven square concrete-filled steel tubes. Among the nine composite beams, one beam, S20-0-2000, was prepared without a deck slab to act as a reference specimen. The chief parameters investigated were the length of the specimen, the compressive strength of the concrete slab, and the effect of the steel tube section type. All beams were tested using the three-point bending test with a concentrated central point load and simple supports. The test results showed that the first crack in the concrete deck slab was recorded at load levels ranging from 50.9% to 77.2% of the ultimate load for composite beams with square steel tubes. The ultimate load increased with increasing the compressive strength of the concrete slab. Shorter specimens were more stiffness than the other specimens but were less ductile. The slip values were equal to zero until the loads reached their final stages, while the specimen S20-55-1100 (short specimen) exhibited zero slip at all stages of the load. The ultimate load of the hollow steel tube composite beam was 13.2% lower than that of the reference beam. Moreover, the ductility and stiffness of the beam were also higher for beams with composite-filled steel tubes.

Keywords: Concrete-filled steel tube (CFST), Lightweight concrete, Composite beam, Perfobond-rib shear connector, Reinforced concrete, Compressive strength, Cracks

¹ University of Al-Qadisiyah, Civil Engineering Department, Al-Diwania, Iraq, e-mail: ms.Khawla.farhan@qu.edu.iq

² Prof., PhD., Eng., University of Al-Qadisiyah, Civil Engineering Department, Al-Diwania, Iraq, e-mail: mohanad.shallal@qu.edu.iq

1. INTRODUCTION

A composite beam makes use of the material properties of both steel and concrete. It is more ductile, has higher strength, and is cheaper than its steel equivalent [1]–[3]. Concrete and steel together as a composite in the construction enhances the ultimate capacity and stiffness. The concrete filling in the steel tube not only prevents the local buckling of the steel but also raises the ductility of the concrete-filled steel tube CFST to higher and better levels up to the ultimate load [4], [5]. Recently, the use of CFST has become common in buildings, bridges, and other structures [6], [7]. The use of CFST members in moment-resisting frames reduces the need for incorporating stiff elements in panel zones and zones that demanded high strain [8]. Bridges with CFST members are estimated to reduce noise and vibration levels compared to those with pure steel members [9]. Also, CFST members have been proven to be cost effective in building structures [10]–[12]. Some usages of CFST members are shown in Fig. 1. Under bending loads, the CFST members perform better than hollow tubes [13]. The lateral confinement by the steel tube adds to the strength of the concrete core [14].

Most previous studies were focused on columns, as they are critical structural elements in high-rise buildings and in areas prone to earthquakes. Other applications, such as flexural members (CFST) are few in the research field. Han [15] did a study on the flexure behavior of CFST. Han tested 36 composite beam specimens that were filled with self-compacting concrete (SCC). Many parameters, such as the ratio of shear span to depth (1.25–6), steel yielding strength (235–282 MPa), sectional types (circular and square), and the ratio of tube diameter or width-to-wall thickness were used in this study. Han found that the CFST filled with SCC are similar to the composite beams that are filled with normal concrete. Moreover, the effect of the shear span to depth ratio was not evident on the square and circular CFST.

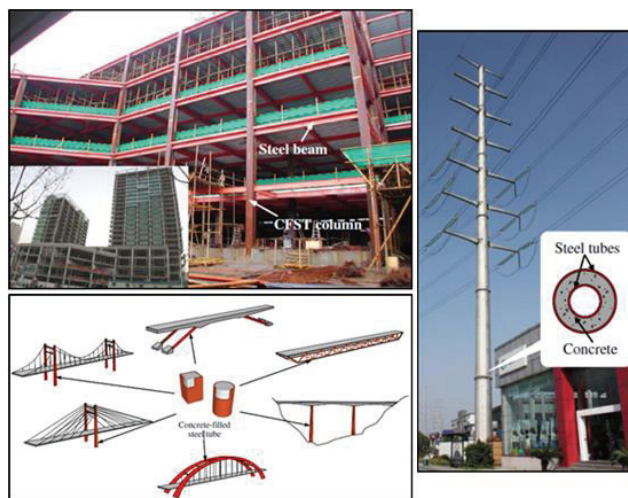


Fig. 1. Applications of CFST composite members.

The flexural capacities of the section were predicted using the four design codes and the method proposed by Han [15], [16]. These methods were compared with the test results by using the proposed method of Han in his study, and the recommendation of design codes. Han's method was the best-predicted method. Shallal [17] tested twelve CFST beams in a study the main objective of which was to determine the maximum load of CFST beams (square and circular) filled with different types of concrete under flexural effect. The study presented an experimental test on the flexural performance of square and circular CFST subjected to bending. From the results of the investigation, it was observed that the maximum moment strength of the CFST was generally higher than that of the corresponding hollow tube beams. This improvement in strength was attributed to the steel confinement for the concrete core which increased the ductility and moment capacity of the composite beam. Zhongqiu [18] tested a composite beam which consisted of a lightweight CFST and a reinforced concrete deck slab. Bending tests were carried out on the beam to study its performance. On the basis of the test results and the assumptions made in the study, the suggested method of calculation was proved by finite element analysis. The results displayed that the composite beam with slab deck and lightweight CFST had good ductility and high capacity. The slip between the CFST and deck slab was ignored in this study. The flexural capacity for such a composite beam by taking into account the yield strength of the steel tube and the concrete strength can be evaluated by the force balance method. The superposition of the deck slab and lightweight CFST caused a higher flexural stiffness in the elastic stage. Mossahebi et al. [19] carried out

experimental studies to understand the performance of a bridge girder consisting of a steel tube filled with concrete and made composite with a concrete deck. The test specimen displayed good ductility and maintained its strength up to the end of the test. Results of this study demonstrated the possibility of using a concrete-filled tube as a bridge girder. The practical application of the new type of CFST girder is presented by Kang et al. [20]. The flexural behavior of the CFST girder that was experimentally tested in this study, varied according to the strength of the filling material. Their application as continuous girders was also evaluated. Results of the test showed that CFST girders had good ductility and maintained their strength up to the end of the loading. Results of this investigation demonstrated the favorable potential of the concrete-filled tube as a bridge girder. Junghyun et al. [21] presented a study on CFST girders. This study included an experimental part that included examining three specimens. The theoretical part included the analysis of the specimens by the finite elements using the Abaqus program, and suggest new equations to find the flexural capacity of a CFST composite girder.

This study presents the investigation of nine composite CFST beams with a deck slab. The parametric study includes different lengths of specimens, section type of the steel tube, and three types of normal concrete used in the concrete deck slab. Perfobond strip was used as a shear connection key in the composite beam, and there are many applications of perfobond connectors that are used to connect the CFST members with the concrete beam. The shape of the perfobond connector that was used in the study is shown in Fig. 2. One mixture of lightweight aggregate concrete was used to fill the hollow beam sections by using clay aggregate (LECA), and three strengths of normal concrete were used in the concrete deck slabs. Not many studies have been conducted on CFST as a flexural member. This study presents the application of this new sort of CFST beam composite with a concrete deck slab. The concrete compressive strength used in filling the steel tube had almost no effect on the flexural strength, therefore, lightweight concrete was used to produce a relatively light composite beam in this study. Nine specimens were designed through which the effect of change in the length of the specimen with fixed depth was evaluated for three specimens. The effect of concrete compressive strength was used in the deck slab where three different mixes were also studied. The effect of the different sections of the steel tube was considered in the study where two specimens type were used, one with a circular section and the other with a square section. The use of a deck slab was also studied where one of the specimens was used without a deck slab and the effect of filling the tube with concrete as one of the specimens formed was without concrete.

2. EXPERIMENTAL PROGRAM

Nine specimens were casted. Each specimen consisted of two main parts: the deck slab and the CFST beam. Seven of the CFST beams were square sections and the other two were circular sections. A summary of specimens is listed in Table 1. The nomenclature of the specimen contains four parts. The first is S or C which refers to a section type (the S means square, and C is for circular). The first number refers to the strength of lightweight concrete inside the tube (20 and 0); zero means that there was no concrete inside the steel tube. The second number refers to the strength of the concrete slab deck (55, 45, and 35 MPa). The last number refers to the total length of specimens: 1100, 2000, and 2900 mm. The dimensions of the steel tube were $150 \times 150 \times 4$ mm, while the dimensions of the circular section were 150 mm in diameter and 3.8 mm in thickness. Fig. 3 shows the details of these specimens. The deck slab dimensions were 450×75 mm which included a steel reinforcement with a diameter of 8 mm. The detail of reinforcement is shown in Fig. 3. The dimensions of the perfobond connector were 50×8 mm which was used as a shear connector between the steel tube and the deck slab. The bottom layer of transverse steel reinforcement passed through the perfobond plate that had a hole of 10 mm. One concrete mix is used to fill the steel tubes (lightweight concrete 20 MPa), while just one square specimen has no infilled concrete (hollow steel tube). The strengths of the concrete deck slab of specimens were (55, 45, and 35 MPa).

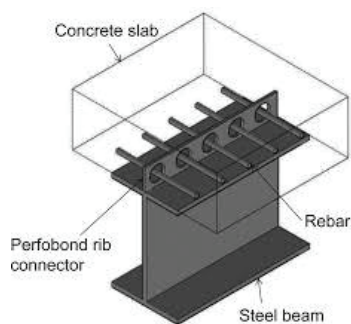


Fig. 2. Composite beam with perfobond connector.

Table-1 Specimen properties.

Specimen label	Effective length	Section type #
S20-55-2000	1800 mm	square
S20-55-1100	900 mm	square
S20-55-2900	2700 mm	square
S0-55-2000	1800 mm	square
S20-45-2000	1800 mm	square
S20-35-2000	1800 mm	square
S20-0-2000	1800 mm	square
C20-55-2000	1800 mm	circular
C20-35-2000	1800 mm	circular

square (150×150×4 mm), circular ($\Phi=150$, $t=3.8$ mm)

3. MATERIAL PROPERTIES

All concrete mixtures contained ordinary Portland cement (Type I), with 10 mm as the maximum size of the coarse aggregate, while the fine aggregate conformed to the requirements of ASTM-C330 specification. The concrete filled in tubes was a lightweight concrete that used gravel with a maximum size of 10 mm as clay aggregate (LECA). Details of concrete mixtures and cubic compressive strengths are summarized in Table 2. The values of yield stress and ultimate tensile strength of the steel tubes, steel reinforcement, and perfbond connector are summarized in Table 3.

4. TEST ARRANGEMENT

All specimens were tested using a universal testing machine. The composite beams were tested under concentrated loads in the middle of the span. Fig. 4 shows a diagram of the device, load cell, and locations of LVDT sensors.

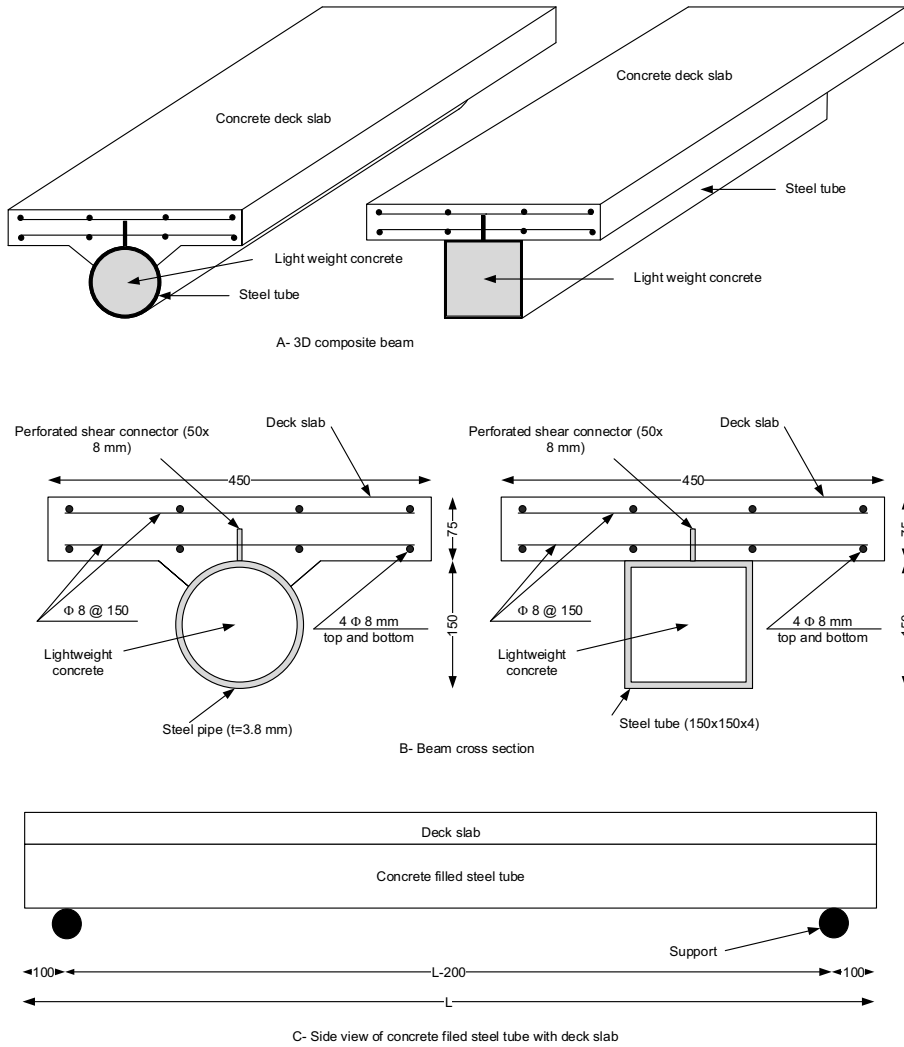


Fig. 3. Scheme of the specimen.

Table-2 Mixing concrete properties.

Mix	Mixing ratio	W/C ratio	Superplasticizer (SP.) %	Compressive strength (MPa)
Lightweight concrete (20 MPa)	1:1.75:0.5	0.3	1	21.85
Normal concrete, M2: 55 MPa	1:1.47:2.2	0.3	0.5	52.17
Normal concrete, M3: 45 MPa	1:1.89:2.84	0.4	0.3	47.93
Normal concrete, M4: 35 MPa	1:2.67:4	0.5	-	35.14

Table 3 Steel members properties.

Component	Yield stress, F_y (MPa)	Ultimate strength, F_u (MPa)
Square tube	390	433
Circular tube	305	391
Reinforcement	464	606
Perfobond connector	357	370

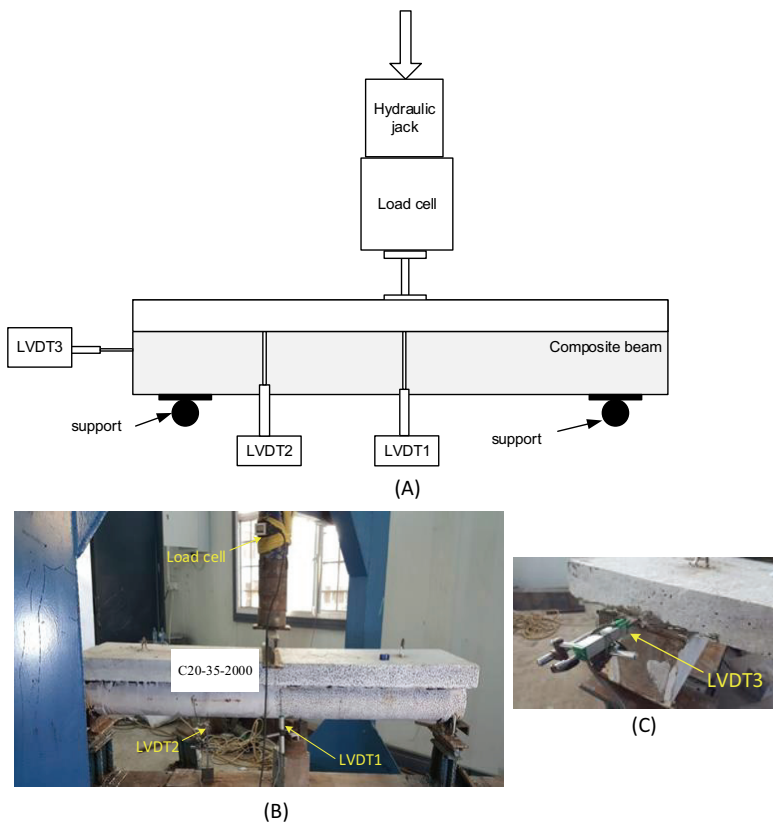


Fig. 4. Scheme of universal test machine and measurement settings.

5. RESULTS AND DISCUSSION

The results obtained from the tests showed that all the specimens failed in the bending test except the specimen S20-55-1100 which exhibited a different behavior in failure. The results are listed in Table 4. Fig. 5 shows some pictures of the test specimen. Ultimate load, cracks, load-deflection curve, and slip at the end of the composite beam were also determined from the tests.

5.1 CRACKS

Cracks inside the steel tube could not be seen during the test. The only cracks that could be seen were those that were in the concrete deck slab. Table 4 lists the loads (P_{crack}) that were recorded when the first crack appeared in the concrete deck slab. The appearance of the first crack in the concrete deck slab was recorded between 50.9% and 77.2% of the ultimate load for the specimens having a square steel tube. It can be concluded that the neutral axis existed in the zone of the steel tube before the load was applied. As a result of cracks in the concrete inside the steel tube, the neutral axis moved upwards within the concrete deck slab. The first crack was noticed in the concrete deck slab of the specimen S0-55-2000 at 106.2 kN, which represents 50.9% of the ultimate load. This percentage was the lowest among all specimens owing to the lack of concrete inside the steel tube. The lack of concrete inside the steel tube made it less stiff compared to the other specimens, so the neutral axis moved to the concrete deck slab in the early stage of the load. Three specimens, S20-35-2000, S20-45-2000, and S20-55-2000, were studied for determining the effect of change in the compressive strength of the deck slab. The first crack was observed in the concrete deck slab of these specimens at loads 126.04, 160.01, and 172.25 kN, respectively, which represents 55.5, 69.2, and 71.7%, respectively, of the ultimate loads of these specimens. It was observed that the specimen which had a high compressive strength imparted a higher stiffness in the specimens and, hence, delayed the crack formation in the concrete deck slab. Three specimens, S20-55-2900, S20-55-2000, and S20-55-1100, were tested for determining the effect caused by the specimen's length. The first crack was observed in the concrete deck slab of these specimens at loads of 105.3, 172.25, and 400.27 kN, respectively, which represent 65.9, 71.7, and 77.2%, respectively, of the ultimate loads of these specimens. These results showed that there existed an inverse relationship between the percentage of the first crack load to the ultimate load and the length of the specimen. The increase in specimen length led to a decrease in the percentage of the crack load. To study the concrete cracks inside the steel tube, a section of the steel tube was cut and removed so that observations of the cracks in the concrete part which was used to fill the steel tube could be

recorded. Fig. 6 shows the cracks in these specimens. At the corners of the square tube, part of the concrete remained adhered to the tube, as shown in Fig. 6. It can be seen that the cracks in the circular section were more in number and had less width than the cracks in the square section. The cracks of the concrete deck slab were fewer than the cracks in the concrete inside the tube. This is normal because higher stress is present near the bottom section. As for the width of the cracks, the cracks of the concrete deck slab were found to be more extensive than the cracks in the concrete inside the steel tube. This explains the presence of a larger number of cracks in this zone as the stress is moderately distributed because of concrete surrounding the steel section. The specimen, S20-55-1100, showed two types of cracks in the concrete deck slab; first, there were flexural cracks, but at the failure point, a crack resulting from the shear stress also started becoming apparent, as shown in Fig. 6.

Table 4. Result of the tested composite beams.

Beam	Ultimate load (Pu) (kN)	P_{crack} (kN)	P_{crack}/P_u (%)	P_{slip} (kN)	P_{slip}/P_u (%)	Stiffness (kN/m $\times 10^3$)
S20-55-2000	240.25	172.25	71.7	215.39	89.7	52.71
S20-55-1100	518.59	400.27	77.2	-	-	74.11
S20-55-2900	159.77	105.30	65.9	112.84	70.6	11.02
S0-55-2000	208.57	106.21	50.9	191.05	91.6	36.87
S20-45-2000	231.31	160.01	69.2	215.04	93.0	44.41
S20-35-2000	227.11	126.04	55.5	116.65	51.4	29.85
S20-0-2000	117.92	-	-	-	-	12.97
C20-55-2000	208.18	159.96	76.8	193.56	93	44.63
C20-35-2000	193.59	116.03	59.9	175.73	90.8	29.75

P_{crack} : load at first crack in the concrete deck.

P_{slip} : load at first slip between the concrete deck and steel tube at the end of the specimen.

5.2 ULTIMATE LOAD AND LOAD-DEFLECTION CURVES

5.2.1 EFFECT OF COMPRESSIVE STRENGTH

Table 4 shows the ultimate load values for all specimens. The results showed that the ultimate load was reduced by decreasing the compressive strength of concrete. Also, the ultimate loads of specimens S20-45-2000, S20-35-2000, and S20-0-2000, were less than the ultimate load for specimen S20-55-2000 by 3.7, 5.5, and 50.9%, respectively. The last percentage, 50.9%, for specimen S20-0-2000 showed a large decrease because of the absence of a concrete deck slab. Therefore, the stiffness was lower than the other specimens. Fig. 7 shows the load-deflection curves owing to the change in the concrete compressive strength in the concrete deck slab. From this figure, a slight difference in the stiffness of the specimens can be noticed except in the case of

specimen S20-0-2000 which showed a significant difference in stiffness because of the absence of a concrete deck slab. Two specimens, C20-55-2000 and C20-35-2000, illustrated the effect of change in the compressive strength of concrete in the deck slab. The ultimate loads of these specimens confirmed that the ultimate load was affected by concrete compression strength as the ultimate load decreased by decreasing the compression strength of concrete. Fig. 8 shows the load-deflection curves. It is evident from the figure that the specimens exhibit the same behavior under the load.

5.2.2 EFFECT OF LENGTH

The results obtained from the tests showed that the beams having different lengths (S20-55-1100, S20-55-2000, and S20-55-2900) with the same properties exhibit different behavior as shown in Fig. 9. The ultimate loads for specimens S20-55-1100, S20-55-2000, and S20-55-2900 were 518.59, 240.25, and 159.77 kN, respectively. These results were as expected because of the difference in lengths of the specimens. The results based on moments were compared, as shown in Fig. 10. The maximum moment for specimens S20-55-1100, S20-55-2000, and S20-55-2900 were 116.68, 108.11, and 107.84 kN, respectively. As shown in Figs. 9 and 10, the beam, S20-55-1100, had more stiffness but less ductility than the two other beams, S20-55-2000, and S20-55-2900. Thus, the beam S20-55-1100 failed by shear and flexure, as shown in Fig. 6, while beams S20-55-2000, and S20-55-2900 failed in flexure.



Fig. 5. Specimens during and after the test.



Fig. 6. Cracks in the test specimens.

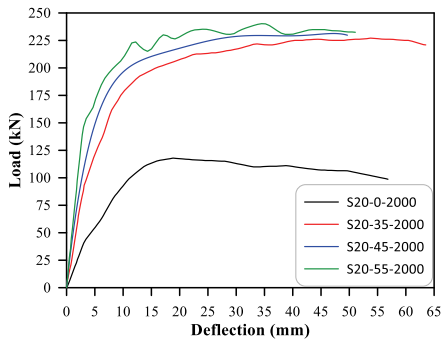


Fig. 7 Effect of concrete compressive strength in specimens of the square tube on load-deflection curves.

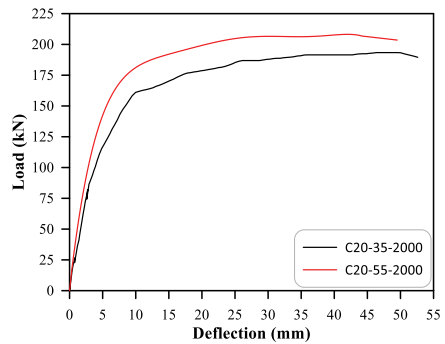


Fig. 8 Effect of concrete compressive strength in specimens of the circular tube on load-deflection curves.

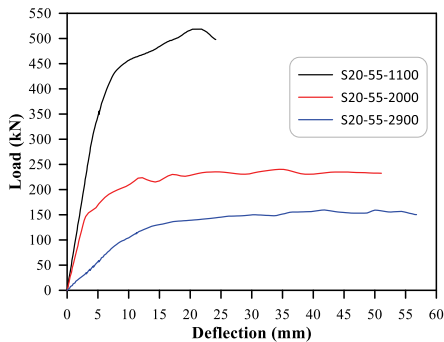


Fig. 9. Effect of specimen length on load-deflection curves.

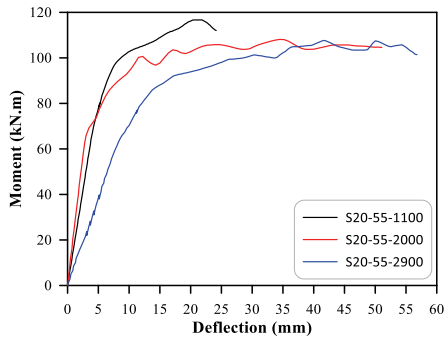


Fig. 10. Effect of specimen length on moment-deflection curves.

5.2.3 EFFECT OF FILLING CONCRETE

In this section, a specimen S20-55-2000 with concrete strength of 55 MPa for a deck slab, and lightweight concrete filled in the tube (21.17 MPa), and another specimen, S0-55-2000 with concrete strength of 55 MPa for a deck slab but with a hollow steel tube was considered. In the mid-span of the beam S0-55-2000, the bottom flange buckled upward as shown in Fig. 11. The ultimate load for the CFST beam S20-55-2000 was 240.25 kN, while for the CFST beam S0-55-2000 it was 208.57 kN, a decrease of 13.2% compared with the reference beam S20-55-2000. Fig. 12 shows the load-deflection curves. It can be seen from the curve that concrete filling the tube significantly increased the ductility. Consequently, the stiffness also increased.

5.2.4 EFFECT OF THE TUBE SECTION TYPE

In this study, a comparison among the CFST beams having different cross-sections of steel tubes (square or circle) has been made. The specimen S20-35-2000's ultimate load, 227.11 kN, was 14.8% higher than the ultimate load of 193.59 kN for specimen C20-35-2000. The specimen S20-55-2000's ultimate load, 240.25 kN, was 13.4% higher than the ultimate load of 208.18 kN for the specimen C20-55-2000. This is shown in Fig. 13.



Fig. 11. Buckling of the bottom flange for specimen S0-55-2000.

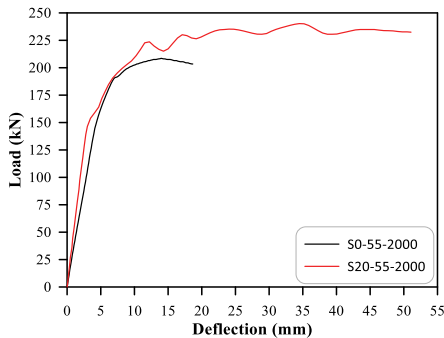


Fig. 12. Effect of filling concrete on load-deflection curves.

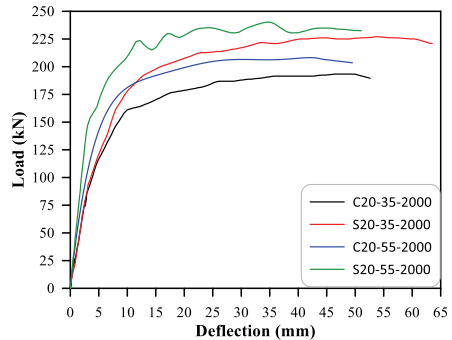


Fig. 13. Effect of tube section type on load-deflection curves.

5.3 SLIP

In this section, the slip between the concrete deck slab and steel tube was measured using LVDT3 at the end of the specimen, as shown in Fig. 4. Slip can be defined as a difference in horizontal movement between the CFST and the concrete deck slab in their interface zone [22], [23]. As shown in Table 4, the slip for all beams began at 90% of ultimate load except two beams, namely, S20-55-2900 which began at 70.6% of ultimate load and S20-35-2000 which began at 51.4% of the ultimate load. Figs. 14-17 show a similar behavior of slip at the end of the beam during increased loads but with slight differences. Figs. 14-17 show that there was no slipping at the end of the beam, and the slip value was zero until the loads reached their final stages. Table 4 shows that the percentage of load in which a slip appeared, ranges from 89.7 to 93.0%, except for three specimens: S20-55-1100, S20-55-2900, and S20-35-2000.

Fig. 14 shows that the specimen S20-35-2000 behaved differently from other specimens as the slip started at an early stage. The slip between concrete and CFST started at 51.4% of the ultimate load and then increased with increasing load until the slip values reached values comparable with the rest of the specimens. This might be due to the decrease in the compressive strength of this specimen. However, specimen C20-35-2000 showed no such behavior, as shown in Fig. 15. Fig. 16 shows that the specimen S20-55-1100 had a higher ultimate load and zero slip. The reason can be attributed to the short length of the specimen and, therefore, curvature was found to be insignificant. Specimen S20-55-2900 showed a behavior similar to the rest of the specimens, but the slip value began at 70.6% of the ultimate load. This might be caused by the length of the specimen compared with the rest of the specimens.

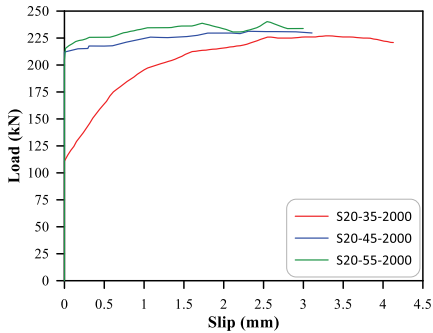


Fig. 14 Effect of concrete compressive strength on load-slip curves.

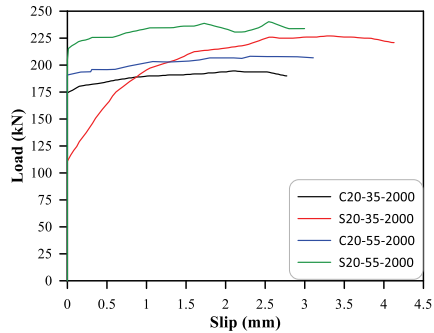


Fig. 15 Effect of section type on load-slip curves.

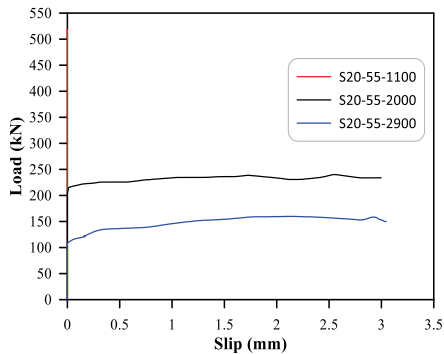


Fig. 16 Effect of specimen length on load-slip curves.

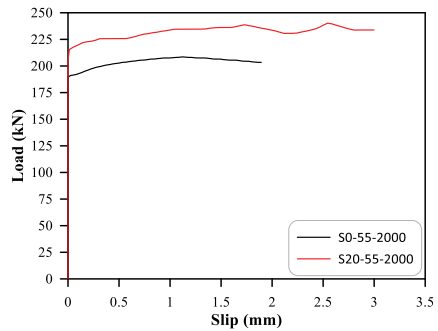


Fig. 17. Effect of filling concrete on load-slip curves.

6 CONCLUSION

The following comments can be drawn as the most important concluding remarks from the experimental work conducted in this research as reported above.

1. The appearance of the first crack in the concrete deck slab was recorded between 50.9% and 77.2% of the ultimate load for the composite beams with a square steel tube.
2. The close examination of the beams after testing showed that the cracks of the lightweight concrete filling in circular steel tubes were higher in number but smaller in width than the cracks in square tubes.
3. The ultimate load capacity of the tested beams was reduced by 3.7% when the compressive strength of the deck slab was decreased from 55 to 45 MPa, while a higher decrease of 5.5% was recorded when the compressive strength was further reduced to 35 MPa.

4. The short beam, S20-55-1100, showed higher initial stiffness than the other beams S20-55-2000, and S20-55-2900, by 28.9% and 85.1%, respectively. However, its deflection corresponding to the ultimate load was lower by 105.0% and 135.1%, respectively.
5. The composite beams with a square steel tube exhibited higher ultimate load and stiffness than those of beams with a circular steel tube.
6. Excluding the three beams S20-55-1100, S20-55-2900, and S20-35-2000, the slip values were zero until the loads reached their final stages. The load at which the slip appeared for all other beams ranged from 89.7 to 93.0% of the ultimate loads. For the beams S20-55-2900 and S20-35-2000, the slip was recorded at 70.6% and 51.4% of the ultimate loads, respectively, while zero slip was recorded for the beam S20-55-1100.
7. The ultimate load capacity for the empty steel tube beam decreased by 13.2% compared with the reference beam. Similarly, the initial stiffness of this beam was lower than that of the reference beam by 30.1%.

REFERENCES

- [1] B.-C. Chen and T.-L. Wang, "Overview of concrete filled steel tube arch bridges in china," *Pract. Period. Struct. Des. Constr.*, vol. 14, no. 2, pp. 70–80, 2009.
- [2] Y. Liu, L. Guo, and Z. Li, "Flexural behavior of steel-concrete composite beams with U-shaped steel girders," in *Proceedings 12th international conference on Advances in Steel-Concrete Composite Structures - ASCCS 2018*, 2018.
- [3] J. Derysz, P. M. Lewiński, and P. P. Więch, "New concept of composite steel-reinforced concrete floor slab in the light of computational model and experimental research," *Procedia Eng.*, vol. 193, pp. 168–175, 2017.
- [4] L.-H. Han, F.-Y. Liao, Z. Tao, and Z. Hong, "Performance of concrete filled steel tube reinforced concrete columns subjected to cyclic bending," *J. Constr. Steel Res.*, vol. 65, no. 8–9, pp. 1607–1616, 2009.
- [5] A. W. Al Zand, W. H. W. Badaruzzaman, A. A. Mutalib, and S. J. Hilo, "Flexural behavior of CFST beams partially strengthened with unidirectional CFRP sheets: experimental and theoretical study," *J. Compos. Constr.*, vol. 22, no. 4, pp. 1-16, 2018.
- [6] S. Fujikura and M. Bruneau, "Dynamic analysis of multihazard-resistant bridge piers having concrete-filled steel tube under blast loading," *J. Bridg. Eng.*, vol. 17, no. 2, pp. 249–258, 2012.
- [7] A. K. Kvedaras, G. Šaučiuvėnas, A. Komka, and A. Juozapaitis, "Design of circular composite beams with a different concrete core considering the effect of concrete in tension," *J. Civ. Eng. Manag.*, vol. 22, no. 1, pp. 118–123, 2015.
- [8] M. Elchalakani, X. L. Zhao, and R. H. Grzebieta, "Concrete-filled circular steel tubes subjected to pure bending," *J. Constr. Steel Res.*, vol. 57, no. 11, pp. 1141–1168, 2001.
- [9] S. Nakamura, Y. Momiyama, T. Hosaka, and K. Homma, "New technologies of steel/concrete composite bridges," *J. Constr. Steel Res.*, vol. 58, no. 1, pp. 99–130, 2002.
- [10] J. Webb and J. J. Peyton, "Composite concrete filled steel tube columns," *Second Natl. Struct. Eng. Conf. 1990 Prepr. Pap.*, p. 181, 1990.
- [11] J. Flor, R. Fakury, R. Caldas, F. Rodrigues, and A. Araújo, "Experimental study on the flexural behavior of large-scale rectangular concrete-filled steel tubular beams," *Rev. IBRACON Estruturas e Mater.*, vol. 10, pp. 895–905, 2017.
- [12] "Performance of concrete filled steel tube (CFST) section: a review," *Int. J. Sci. Res.*, vol. 4, no. 11, pp. 645–647, 2015.
- [13] L.-H. Han, W. Li, and R. Bjorhovde, "Developments and advanced applications of concrete-filled steel tubular (CFST) structures: Members," *J. Constr. Steel Res.*, vol. 100, pp. 211–228, 2014.
- [14] Y.-F. An, L.-H. Han, and C. Roeder, "Flexural performance of concrete-encased concrete-filled steel tubes," *Mag. Concr. Res.*, vol. 66, no. 5, pp. 249–267, 2014.

- [15] L.-H. Han, H. Lu, G.-H. Yao, and F.-Y. Liao, "Further study on the flexural behaviour of concrete-filled steel tubes," *J. Constr. Steel Res.*, vol. 62, no. 6, pp. 554–565, 2006.
- [16] L.-H. Han, "Flexural behaviour of concrete-filled steel tubes," *J. Constr. Steel Res.*, vol. 60, no. 2, pp. 313–337, 2004.
- [17] M. A. Shallal, "Flexural behavior of concrete-filled steel tubular beam," in *2018 International Conference on Advance of Sustainable Engineering and its Application (ICASEA)*, 2018, pp. 153–158.
- [18] Z. Fu, Q. Wang, Y. Wang, and B. Ji, "Bending performance of lightweight aggregate concrete-filled steel tube composite beam," *KSCE J. Civ. Eng.*, vol. 22, no. 10, pp. 3894–3902, 2018.
- [19] N. Mossahebi, A. Yakel, and A. Azizinamini, "Experimental investigation of a bridge girder made of steel tube filled with concrete," *J. Constr. Steel Res.*, vol. 61, no. 3, pp. 371–386, 2005.
- [20] J. Y. Kang, E. S. Choi, W. Chin, and J. W. Lee, "Flexural behavior of concrete-filled steel tube members and its application," *Int. J. Steel Struct.*, vol. 7, pp. 319–324, 2007.
- [21] J. Cho, J. Moon, H.-J. Ko, and H.-E. Lee, "Flexural strength evaluation of concrete-filled steel tube (CFST) composite girder," *J. Constr. Steel Res.*, vol. 151, pp. 12–24, 2018.
- [22] M. A. Shallal, A. M. K. Al Musawi, and F. I. Muss, "Non-linear analysis of continuous composite beam subjected to fire," *International Journal of Civil Engineering and Technology (IJCET)*, vol. 9, pp. 521–532.
- [23] M. Shallal and A. M. K. Al Musawi, "Non-linear analysis of composite beam subjected to fire," *J. of Engineering and Applied Sciences*, vol. 13, pp. 9643–9650.

LIST OF FIGURES AND TABLES:

Fig. 1. Applications of CFST composite members.

Fig. 2. Composite beam with perfobond connector.

Fig. 3. Scheme of the specimen.

Fig. 4. Scheme of universal test machine and measurement settings.

Fig. 5. Specimens during and after the test.

Fig. 6. Cracks of the testing specimens.

Fig. 7 Effect of concrete compressive strength in specimens of the square tube on load-deflection curves.

Fig. 8 Effect of concrete compressive strength in specimens of the circular tube on load-deflection curves.

Fig. 9. Effect of specimen length on load-deflection curves.

Fig. 10. Effect of specimen length on moment-deflection curves.

Fig. 11. Buckling of the bottom flange for specimen S0-55-2000.

Fig. 12. Effect of filling concrete on load-deflection curves.

Fig. 13. Effect of tube section type on load-deflection curves.

Fig. 14 Effect of concrete compressive strength on load-slip curves.

Fig. 15 Effect of section type on load-slip curves

Fig. 16 Effect of specimen length on load-slip curves.

Fig. 17. Effect of filling concrete on load-slip curves.

Table-1 Specimen properties.

Table-2 Mixing concrete properties.

Table 3 Steel members properties.

Table 4. Result of the tested composite beams.

